Corrosion Resistance Studies of Mild Steel by 2-(Benzylidene-Amino)-Benzenethiol Inhibitor in Sea Water Solution

S. Sulochana[1], A. John Amalraj[1*], S. Ignatius Arockiam[2] and S. S. Syed Abuthahir[3]

[1]PG and Research Department of Chemistry, Thanthai Periyar Government Arts and Science College (Autonomous), Tiruchirappalli – 620 023, Tamilnadu, India.

[2]PG and Research Department of Chemistry, GTN Arts College (Autonomous), Dindigul- 624005,Tamil Nadu, India

[3]PG and Research, Department of Chemistry, Jamal Mohamed College (Autonomous), Tiruchirappalli – 620 020, Tamil Nadu, India.

amalrajevr@gmail.com

Abstract

The resistance to deterioration ability of an inhibitor, primarily 2-(benzylidene-amino)-benzenethiol, which influences the deterioration of mild steel dished in sea water was studied using a mass loss approach, an electrochemical study, in addition to AC impedance spectra. This was done in order to determine how an inhibitor influences the deterioration of mild steel dished in sea water. AFM, FTIR, SEM, and EDAX are all employed to understand the essence of the surface morphology. According to the magnitudes of the mass loss methodology spectacle, the presence of 250 ppm of the inhibitor in seawater has an inhibition efficiency (IE) of 82.37 percent. Polarization is an examination of abilities that demonstrate that strategy, such as cathodic inhibitors. The incredulous cover rising can be seen on the AC impedance spectrum of the mild steel. The fact that the protective coating has a chemical with the formula Fe^{2+}-inhibitor has been confirmed by FTIR, SEM, EDAX, and AFM.

Keywords: Inhibitor, Sea water, mild steel, FTIR, SEM EDAX, AFM

1. Introduction

Mild steel is one of the metals that is used the most often in construction, food processing, power generation, chemical production, and other industrial applications. This is due to the fact that mild steel may be used in a wide variety of contexts. [1] As a result of the great demand, a significant quantity is created (made) [2, 3]. It is sturdy, resistant to damage, and has remarkable mechanical strength. Organic inhibitors have been proven to be among the most effective anti-corrosion

remedies by researchers and engineers [4]. Organic inhibitors attach themselves to the surface of the metal and create a protective coating. This coating prevents oxygen and water from accessing the metal, which would otherwise lead to corrosion. The presence of p-electrons in aromatic rings and heteroatoms (N, S, O, and P) in the molecular structure of organic inhibitors is responsible for their adsorption and film-forming capabilities [5, 6]. A portion of the building may have a cathodic zone because it is submerged at the saltwater/air contact and is thus more aerated than the lower portions, which are anodic zones. This is because the bottom parts are anodic zones. We are of the opinion that the primary mechanisms that are responsible for the production of the corrosion product layers on the anodic and cathodic zones have not been sufficiently researched [7]. Corrosion inhibitor for mild steel in sea water: computational and electrochemical experiments [8] by Abdelshafeek et al. found that Vicia faba peel extracts containing fatty acids moieties were both cost-effective and ecologically benign. Atan et al. looked examined the usefulness of moringa leaf extract (Moringa Oleifera) as a green material [9] when it comes to reducing corrosion in carbon steel. The efficiency of a polyaspartic acid derivative composite in preventing the corrosion of carbon steel in the presence of saltwater was examined by Gao et al. using a polyaspartic acid derivative composite. In a sodium chloride solution, Mohamed Kasim Sheit and his colleagues tested the anticorrosion characteristics of mild steel. [10] Researchers used a compound known as 5-acetyl-3-phenyl-2, 6-dipyridin-2-yltetrahydropyrimidin-4 (1H)-1 as an inhibitor. Using a thiophenol derivative inhibitor, researchers under the direction of Raja T. et al. [11] examined the electrochemical behaviour of carbon steel while submerged in a sodium chloride solution. In an experiment using simulated seawater, Bokati, K. S., et al. [12] investigated the effects of 1H-benzotriazole, sodium molybdate, and sodium phosphate on the corrosion of copper, mild steel, and copper-mild steel that had been galvanically linked. In order to determine the synergistic effect that Mangifera indica leaf extract and zinc ions have on preventing the corrosion of mild steel in simulated saltwater, Ramezanzadeh, M., et al. undertook a computational and electrochemical investigation [13]. The concept of determining the multiplicative qualities of the inhibitor is now the notion that is leading the pack. Infrared, scanning electron microscopy, electron dispersive X-ray, and atomic force microscopy were all used in the course of the research that was conducted on a specific amino benzoic acid multipart that controls the rate of zinc metal deterioration when it is submerged in seawater [14-15]. In this particular line of investigation, we made use of the mass defeat approach, electrochemical analyses, and AC impedance spectra.

2. Experimental Procedure

2.1. Preparation of the mild steel specimens

The mild steel sample has the following chemical composition: 0.1% carbon, 0.026% sulphur, 0.06 phosphorus, 0.4% manganese, and the rest iron. The specimen, which measured 1 cm x 4 cm x 0.2 cm, was polished to a mirror-like finish. Before using mild steel in the weight-loss process, oil must be removed from it with acetone. Working electrodes for potentiostatic polarization experiments were mild steel samples that had been covered in Teflon. 1 square cm made up the exposed cross section. The electrode was polished to a mirror sheen, then the oil was removed from the surface using ethanol. [16].

2.2. Preparation of Stock Solution

At each and every location where it was required, stock solutions were prepared using sea water. Before being added to the quantity of seawater of choice, 2-(benzylidene-amino)-benzenethiol was first dissolved in an insignificant amount of ethanol in order to make available the prerequisite concentration for the stock solution. Afterwards, the desired concentration of inhibitor stock solution had been added to the seawater solution.

2.3. Mass loss and Corrosion Rate Approach

The method of mass loss was carried out in a manner that was compliant with the protocol. On the first day of the mass loss procedures, specimens of mild steel were submerged in different concentrations of seawater and 2-(benzylidene-amino)-benzenethiol for a period of one day (50 ppm -250 ppm). After being confined for a period of twenty-four hours, the subject of the test is released, subjected to a series of drenchings with water, dried off, and then weighed [17-18]. The following equation (1) is used at this point in order to estimate how effective the inhibition will be:

$$\text{IE}\ (\%) = \frac{W_0 - W_1}{W_0} X100 \qquad (1)$$

Where,

W 1 is the rate of corrosion when there is no inhibitor. and

W2 is the corrosion rate when the inhibitor is present.

During 24 hours, duplicate mild steel specimens were immersed in 100 ml of sea water with varying doses of the 2-(benzylidene- amino)-benzenethiol inhibitor. The samples were removed from the water after 24 hours, cleaned with running water, dried, and weighed. The following

equation (2) was used to determine corrosion rates from observations of weight changes in the specimens:

$$\text{Corrosion rate} = \frac{87.6 \text{ x Loss in weight}(\text{mg})}{\text{Surface area of the specimen}(\text{dm}^2)\text{x}} \mu\text{m / y} \qquad (2)$$
$$\text{Period of immersion}(\text{Hr}) \times \text{Density}$$

2.4. Characterization Techniques

The surface morphological and topological image features of the prepared mild steel were analyzed using a Zeiss Sigma model: FEI Quanta 250. To determine the functional groups of the Mild Steel, FTIR analysis was conducted using Spectrum One model spectrometer from Perkin Elmer. The annexed Energy Dispersive X-ray analyzer determines the composition of the expected elements in the sample. In addition, anticorrosion analysis was also discussed.

3.Results and Discussion

3.1. Analysis of the Mass loss and Corrosion rate

Table 1 presents the findings of an experiment in which different amounts of corrosion inhibitor were applied to mild steel and then immersed in salt water. According to the findings, the effectiveness of the inhibition increases as the concentration of the inhibitor grows. The higher efficacy of inhibition may be attributed to the blocking action that is based on adsorption and occurs on the surface of the metal. This is due to the fact that corrosion inhibitors often include nitrogen atoms in addition to double bonds. In addition to this, the delocalized electrons of the chemical help to strengthen its inhibitory effectiveness. Several analyses have demonstrated that these results are completely congruent, and as a direct result, a surface layer forms on mild steel. Testing mild steels in seawater with and without a 2-(benzylidene-amino)-benzenethiol inhibitor produced using the weight loss technique and comparing the findings allows for the determination of the corrosion rates (CR) and inhibition efficiency (IE) of these materials [19]. According to the results, using 250 ppb of 2-(benzylidene-amino)-benzenethiol can result in an inhibitory efficiency of 80.9%. It has been demonstrated that a higher concentration of dibutyl sulphide inhibits corrosion more effectively than a lower one [20]. This is due to the fact that a high proportion of the inhibitor covers a greater surface area, slowing the breakdown of zinc metal. The enhanced inhibitory efficacy provided by nitrogen and sulphur atoms may be a result of their ability to donate electrons. The monitoring's findings are consistent with those of numerous previous examinations [21].

Table 1

Corrosion rates (CR) and inhibition efficiency (IE%) mild steel is submerged in sea water with and without inhibitor systems at varied weight loss concentrations.

Blank	**2 - (Benzylidene - Amino) - Benzenethiol (ppm)**	**CR (mdd)**	**IE (%)**
Sea Water	----	36.23	----
	50	29	24.56
	100	21.92	32.06
	150	16.86	46.2
	200	12.34	61.71
	250	9.9	82.37

3.2. Analysis of the potentiodynamic polarization study's findings

Three-terminal cells were used for the polarisation analysis. The pedestrian terminal is made of a lightweight metallic substance, with a cathode exposed to view in a standard 1 cm^2 area and the left side coated in a red finish. A platinum foil of quadrilateral shape was substituted for the original cathode, which was a calomel anode that had been soaked. The conditions at the counter terminal morphed into a massive cathode that mimicked the appearance of a live terminal. The platinum cathode and activity terminal were completely free of inhibitor after being submerged in seawater. The experimental response was linked to a soggy calomel cathode through a sour extension [22]. Consumption potential (Ecorr) and the Tafel slants ba and bc may be calculated from a plot of E against I (log current).

The potentiodynamic polarization investigation lends credence to the hypothesis that the corrosion inhibitor resulted in the formation of a protective layer on the surface of the mild steel. Tafel diagrams are used to do the calculations necessary to determine the corrosion potential (Ecorr), the current density (Icorr), and the potential difference (V_{def}) (b_a, b_c). Extrapolating the linear Tafel segments of the anodic and cathodic curves to the corrosion potential allowed for the calculation of the corrosion current density (Icorr). During the process of preventing corrosion, a polarisation research revealed that mild steel produces a protective layer. As a protective coating

forms on the surface of mild steel, the linear polarisation resistance (LPR) of the steel goes up while the corrosion current (I_{corr}) goes down [23-24].

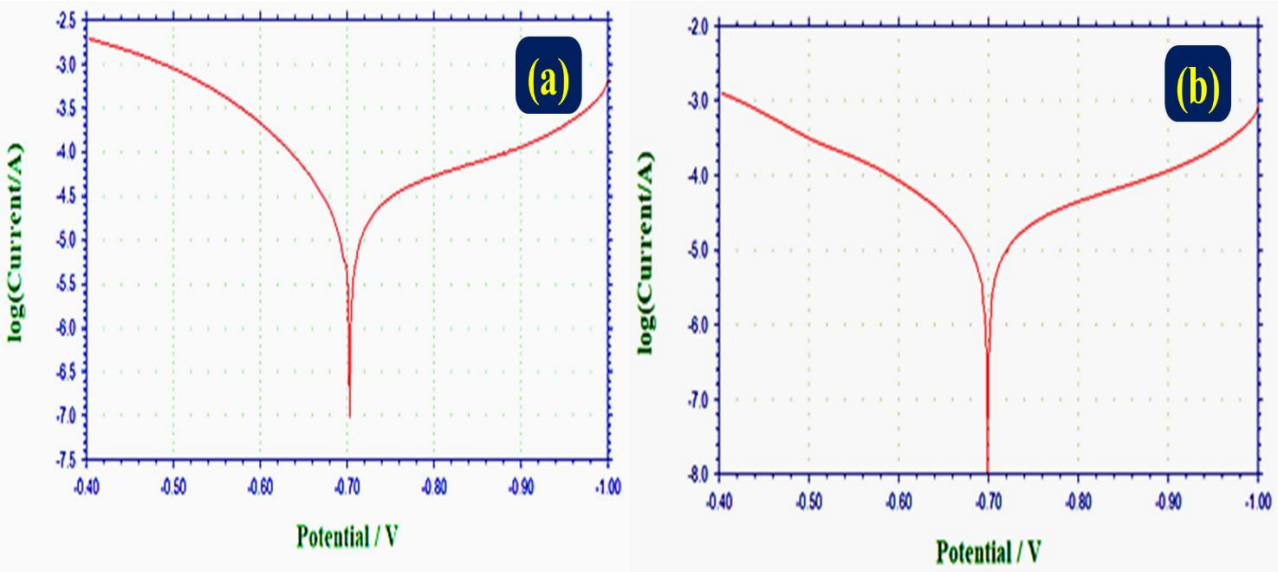

Figure 1 Polarization curves of mild steel immersed in test solutions (a). Sea Water (blank) (b). Sea Water + 250 ppm of 2-(benzylidene-amino)-benzenethiol

Figure 1 (a,b), displays the potendiodynamic polarization curves of mild steel in sea water together with the inhibitory efficiency (IE) of the material both with and without an inhibitor. Table 2, presents the corrosion values for your perusal. Mild steel exhibited a corrosion potential of -0.703 mV against SCE when it was put in an environment with sea water. When 250 ppm of 2-(benzylidene-amino)-benzenethiol was added, the corrosion potential was moved to the favourable side, reaching a value of -0.699 mV against SCE. This result can be seen up above. The mild steel surface's anodic areas are what particularly encourage the development of the protective layer. Due to the creation of a Fe^{2+}-inhibitor complex at the anodic sites on the surface of the mild steel, this film may be able to regulate the anodic reaction of dissolution [25].

Table 2

Potentiodynamic polarisation technique for mild steel corrosion characteristics in sea water and inhibition efficiencies (IE) in the absence and presence of inhibitor system.

Systems	**E_{corr} vs**	**I_{corr}**	**b_a**	**b_c**	**LPR**
	SCE (mV)	**(A/cm^2)**	**(mV/dec)**	**(mV/dec)**	**(ohm cm^2)**
Blank (Sea water)	-0.703	2.905×10^{-5}	0.109	0.256	1146
Sea Water + 250 ppm of inhibitor	-0.699	1.8667×10^{-5}	0.125	0.202	2020

Moreover, the corrosion current drops from 2.905×10^{-5} A/cm^2 to 1.8667×10^{-5} A/cm^2, and the LPR value rises from 1146 ohm cm^2 to 2020 ohm cm^2. Polarization analysis therefore validates the development of a protective coating on the mild steel surface [26].

3.3. Analysis of AC impedance spectra

AC impedance studies were conducted at a CHI- electrochemical work station utilising an impedance model 660A. The cell setup was typical for polarisation experiments. It was required that the system take between 5 and 10 minutes to achieve steady state, when an open circuit potential is present. On top of this resting potential, a 10 mV alternating current (AC) potential was applied. Alternating current (AC) frequencies between 100 kilohertz and 100 megahertz were used to determine the real and imaginary components of the cell's resistance, expressed as ohms. It was possible to calculate the double layer capacitance and the charge transfer resistance. In order to calculate C_{dl} values, the following equation (3) was used.

$$C_{dl} = \frac{1}{2 \text{ x } 3.14 \text{ x } R_t \times f_{max}} \qquad (3)$$

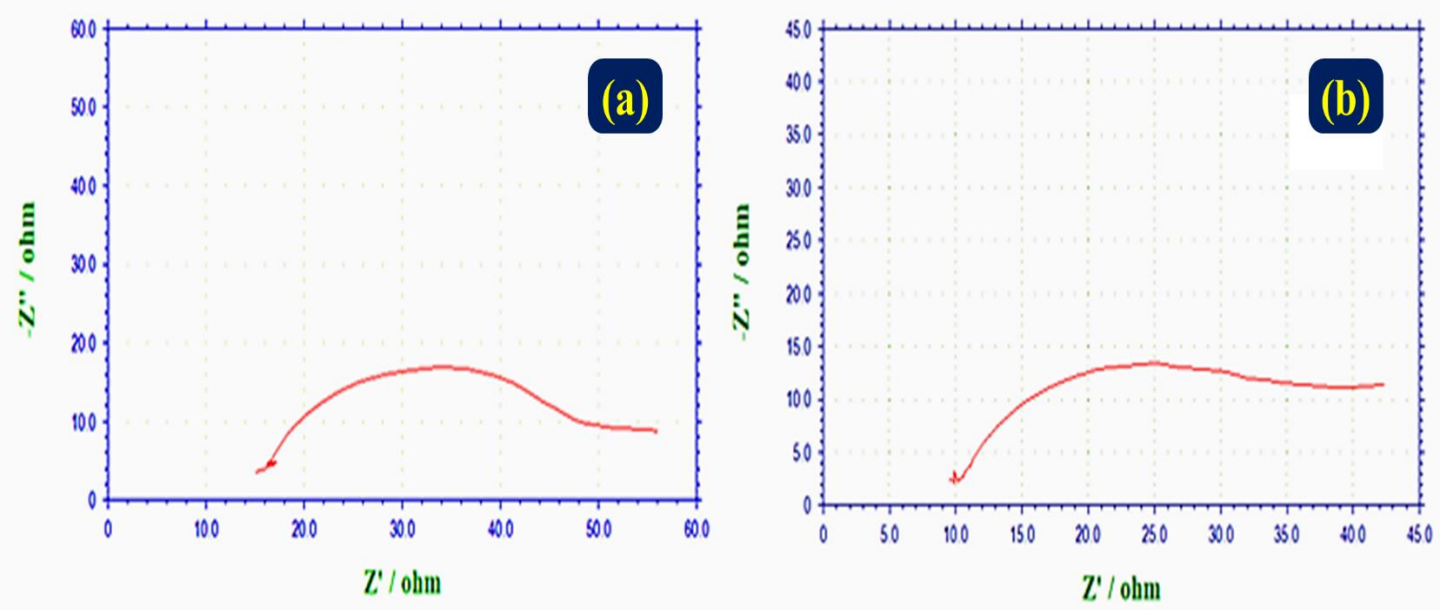

Figure. 2 (a). AC impedance spectra of mild steel immersed in sea water (blank)
(b). 250 ppm of 2-(benzylidene-amino)-benzenethiol

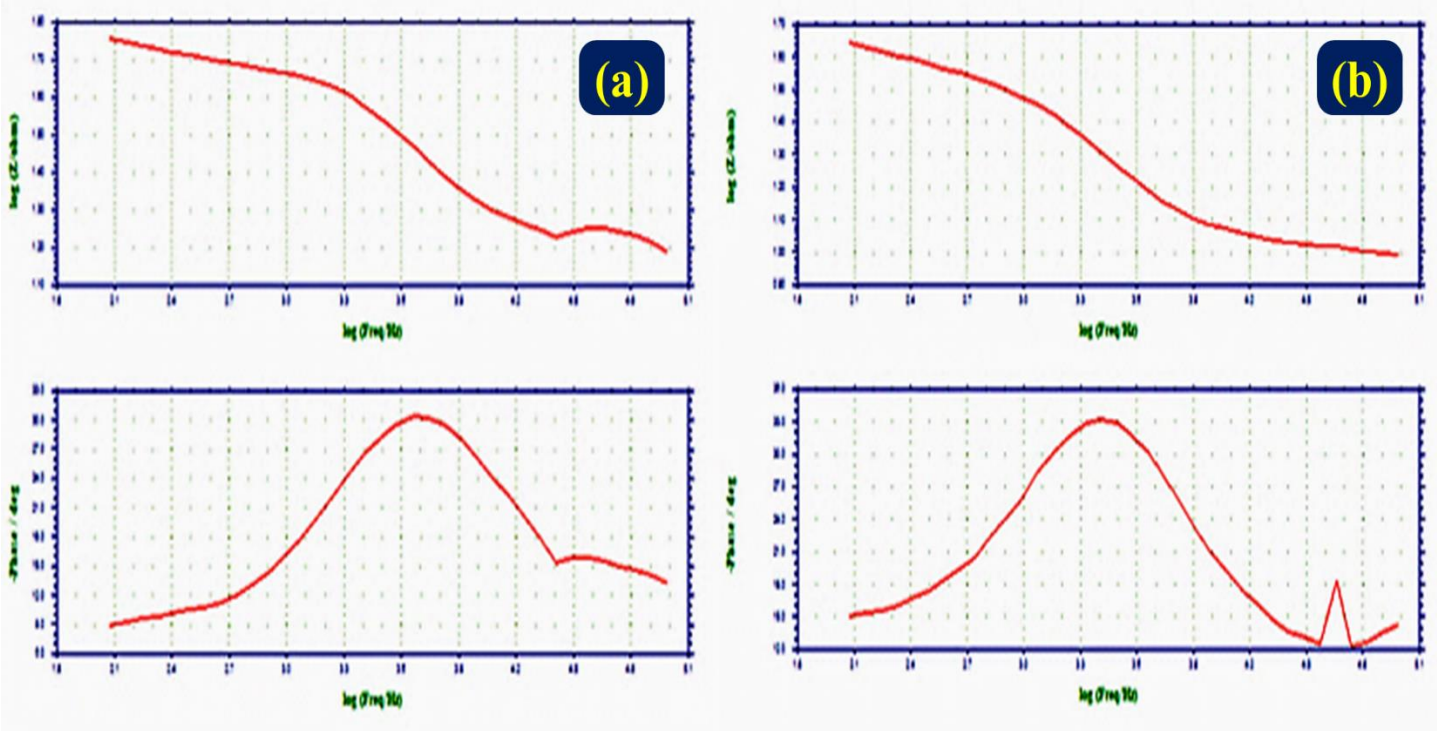

Figure 3 Bode plot of AC impedance spectra of mild steel immersed in (a). Sea water (blank) (b). Sea water and 250 ppm of 2-(benzylidene-amino) - benzenethiol.

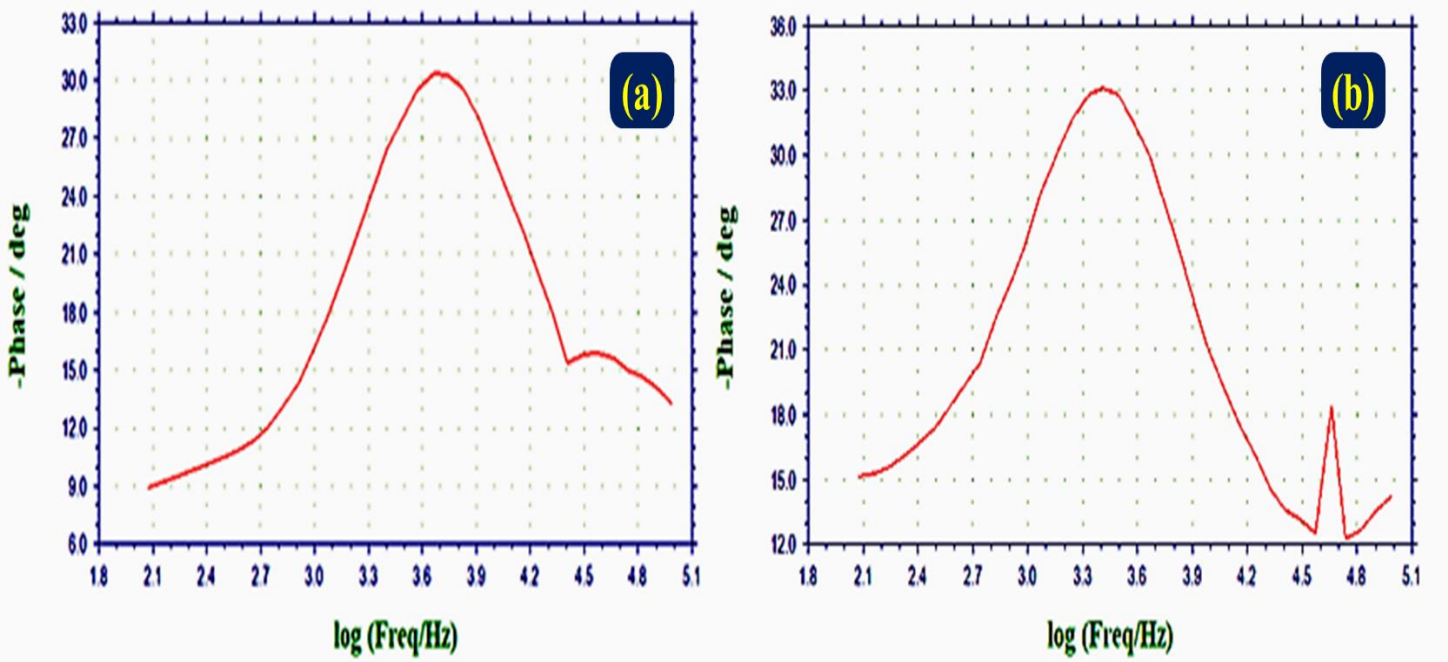

Figure 4 The phase angle of AC impedance spectra of mild steel immersed in
(a) Sea water (blank) (b) Sea water and 250 ppm of 2-(benzylidene-amino)- benzenethiol.

AC impedance spectra have been used to show how a protective layer is formed on the surface of mild steel. This barrier serves as a deterrent to corrosion. If a protective coating forms on the surface of the mild steel, the values for charge transfer resistance (Rt), double layer capacitance (Cdl), and impedance log (z/ohm) will all increase. The AC impedance spectra of mild steel submerged in sea water with and without the inhibitor 2-(benzylidene-amino)-benzenethiol are depicted in Figure 2 (a-b) (Nyquist plots), Figure 3 (a-b) (Bode plots), and Figures 4 (a-b) (Bode plots), respectively (Phase angle). Table 3, which is shown below, provides the numerical information. When the inhibitor 2-(benzylidene-amino)-benzenethiol is given to the system at a concentration of 250 ppm, charge transfer resistance (Rt) increases from 32.48 cm^2 to 41.36 cm^2. At the same time, the Cdl value falls from 68.0211 $x10^{-6}$ F cm^{-2} to 53.4945x 10^{-6} F cm^{-2} [27]. Because of the increase in impedance, the logarithm of the z/ohm, which is a number that is used to show the impedance value, has risen from 0.572 to 0.644. This indicates that the impedance value has increased. As a consequence of this, the value of the phase angle likewise rises, moving from 30 to 33 degrees as a direct consequence [28-29]. These facts lead us to the possibility of reaching the conclusion that the surface of the mild steel, over the course of time, develops a protective coating.

Table 3

AC impedance spectra of mild steel in sea water without and with inhibitor system.

Systems	Nyquist plot		Bode plot
	R_t	C_{dl}	Impedance
	Ω cm^2	F cm^{-2}	Lg (Z ohm^{-1})
Blank (Sea Water)	32.48	68.0211×10^{-6}	0.572
Sea Water + 250 ppm of 2 - (benzylidene-amino) - benzenethiol	41.36	53.4945×10^{-6}	0.644

3.4. Analysis of FTIR spectra

The FTIR spectra of the inhibitor compounds are analysed in order to determine the level of interaction between the molecules and the metal surface. Used for research on the protective layer that develops on mild steel after being heated. The structure of 2-(benzylidene-amino)-benzenethiol is shown in figure 5a. The FTIR spectrum of 2-(benzylidene-amino) - benzenethiol in its purest form is shown in figure 5a, which uses KBr as the reference medium [30]. The C-N stretching frequency may be seen in plain view with a frequency of 1688.92 cm^{-1}. At 1593.76 cm^{-1}, one may see a maximum that is caused by the equation C=N. The stretching frequency of CH, which occurs at 3365.68 cm^{-1}, is the cause of this peak in the spectrum. The SH stretching frequency is calculated to be 1013.46 cm^{-1}, as far as I can ascertain. The C=S stretch has a frequency of 1157.91 cm^{-1} according to our observations [31]. The signal that is connected with aromatic C=C is received at a frequency of 1285.57 cm^{-1}.

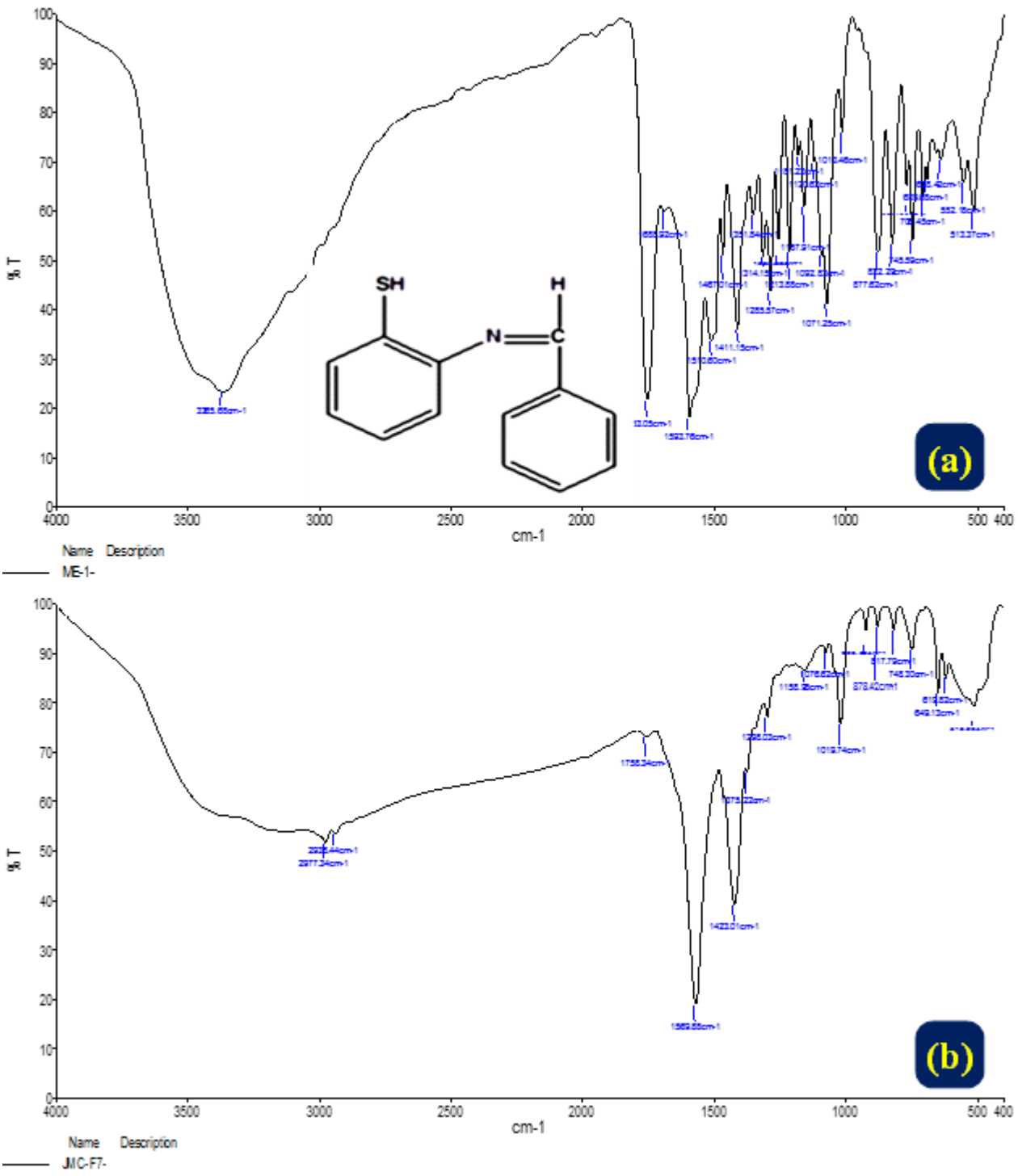

Figure 5 FTIR spectrum of (a) Pure 2-(benzylidene-amino)-benzenethiol (b) The mild steel surface after immersion in sea water solution containing 250 ppm of 2-(benzylidene-amino)- benzenethiol

The FTIR spectrum (KBr) in figure 5b reveals that a coating develops on the surface of the mild steel when it is exposed to salt water and 250 ppm of 2-(benzylidene-amino)- benzenethiol. This is shown by the fact that the coating is visible. The C-N stretching has dropped to 1569.88 cm^{-1} from its previous value of 1688.92 cm^{-1}. The C=N stretching frequency shifts as a direct consequence of this, moving from 1593.76 cm^{-1} to 1596.88 cm^{-1}. The frequency at which CH stretches has decreased from 3365.68 cm^{-1} to 2977.34 cm^{-1} as a result of this alteration. The previous frequency of SH stretching was 1013.46 cm^{-1}, however it has now been raised to the current value of 1019.74 cm^{-1}. The C=S stretching frequency was adjusted upward to 1158.95 cm^{-1}, from 1157.91 cm^{-1} before [32]. The former peak, which was caused by aromatic C=C and was located at 1285.57 cm^{-1}, has shifted to a new site at 1298.03 cm^{-1}. A new peak appears in the region of 619.82 cm^{-1} as a result of the formation of a complex by zinc on the surface of mild steel [33]. Because of the interaction between the sulphur and nitrogen atoms in 2-(benzylidene-amino) - benzenethiol, a Fe^{2+} - inhibitor complex has been generated on the surface of mild steel. The interpretation of the FTIR spectrum, as a result, leads one to the conclusion that the barrier film is composed of a mixture of Fe^{+2} that is inhibitive [34].

3.5. Morphological Analysis of Mild Steel

SEM images are used to evaluate the surface of mild steel. Scanning electron micrographs of mild steel samples submerged in saline water for one day with and without an inhibitor system are shown in figure 6 (a-c), respectively. Polished mild steel serves as a control sample in the scanning electron micrograph of smooth material surface illustrated in figure 6 (a). This information shows that no inhibitor complex or corrosion products have formed on the surface of the mild steel. Scanning electron micrograph of mild steel submerged in salt water reveals surface roughness figure 6b, indicating the presence of heavily corroded mild steel [35]. Nevertheless, as is evident in figure 6c, the number of corroded sections is decreasing, suggesting that the addition of an inhibitor (250 ppm of 2-(benzylidene-amino)-benzenethiol) slows down the rate of corrosion. When an insoluble compound forms on the surface of mild steel, corrosion is almost completely prevented. A microscopic film of inhibitors forms on the surface in the presence of 2-(benzylidene-amino) - benzenethiol. This layer's job is to effectively regulate how quickly mild steel dissolves [36].

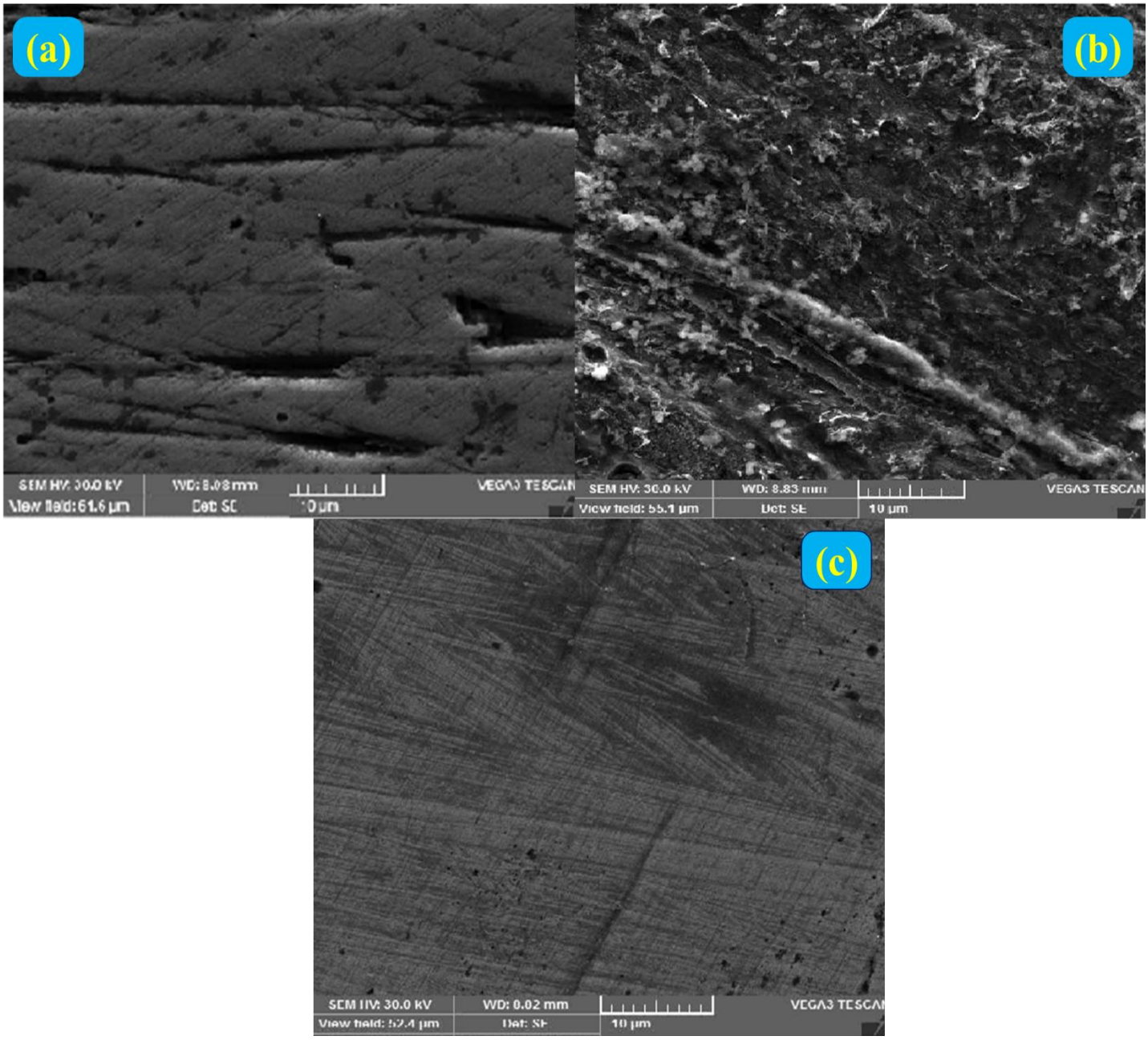

Figure 6 SEM analysis of (a) Mild steel, (b) Mild steel immersed in sea water (blank), (c) Mild steel immersed in sea water and 250 ppm of 2-(benzylidene-amino)-benzenethiol.

3.6. EDAX Analysis of Mild Steel

The elements that were present on the surface of the mild steel metal before and after treatment with the inhibitor solution were identified by analysing the EDAX spectra after treatment. On the surface of mild steel, both with and without an inhibitor system, EDAX investigations were carried out. This was done so that this could be accomplished. The EDAX spectrum of zinc metal is shown here in Figure 7a for your viewing pleasure. The specimen of mild steel has a number of components that may be identified as significant peaks on the spectrum. The EDAX spectrum of mild steel as it is immersed in a saltwater solution may be seen in Figure 7b. Corrosion caused by exposure of mild steel to salt water, as seen by a drop in the strength of the Fe signal and an increase in the intensity of the O signal at its characteristic maxima [37]. The EDAX spectrum of mild steel in a sea water solution containing 250 ppm of 2-(benzylidene-amino)-benzenethiol is shown in Figure 7c. It illustrates that the strength of O signals is reducing while the intensity of Fe signals is growing, which is a phenomenon that is diagnostic of the existence of a second line because it shows that the strength of O signals is declining while the intensity of Fe signals is increasing. According to the results of these tests, the surface of the mild steel is mostly made up of carbon, manganese, copper, and iron. The origin of this layer can be traced back to the inhibitor system [38].

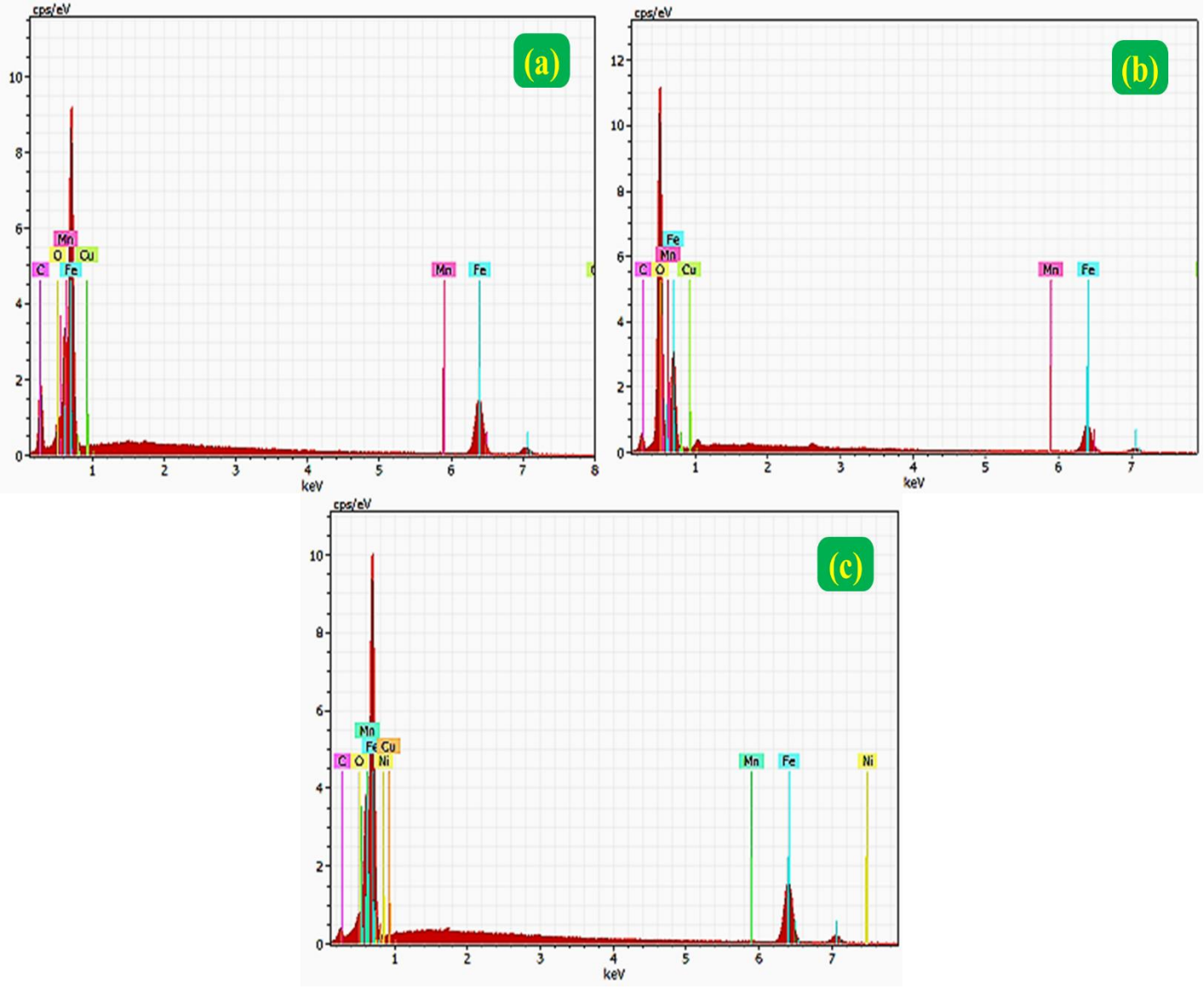

Figure 7 EDAX spectrum of (a) Mild steel specimen (control), (b) Mild steel specimen after immersion in sea water solution (blank), (c) Mild steel specimen after immersion in sea water + 250 ppm of 2- (benzylidene-amino) - benzenethiol

3.7. Topological Analysis of Mild Steel

Topological image was utilized in order to investigate the effects of salt water on the surface roughness of mild steel as well as the presence of inhibitor chemicals on the surface roughness of polished mild steel. Both of these investigations were carried out in order to learn more about surface roughness. The measured values of Sp, Sq, Sa, and Sy for the reference surface of polished mild steel are (85.65, 20.21, 16.20, and 162.21) nm, which indicates a more uniform surface figure 8a. On the other hand, the measured values for the blank are (1315, 277.53, 217.24, and 2348) nm, which indicates a higher level of surface roughness. These results can be found in table 4 measured values of Sp, S. In addition, studies have shown that the roughening of the surface of exposed mild steel is caused by the corrosion of metals in the aqueous solution of salt water figure 8b. When the average roughness (Sa) value drops from 47.21 nm in the inhibitor to 217.24 nm in the blank when corrosion inhibitor is present in sea water, it is clear that inhibitors are effective in preventing corrosion [39-40]. This is demonstrated when the value drops from 47.21 nm in the inhibitor to 217.24 nm in the blank. The formation of a dense protective coating, which is responsible for the surface's better look, may be inferred from a difference in these characteristics that is large enough to be considered suggestive of such production figure: 8c. It was possible to avoid a deposit of the corrosion byproduct onto the surface of the mild steel [41-42]. These findings are supported by the results of the optical cross section study, which demonstrate significant alterations. On the surface of the mild steel, a protective coating was placed, which protected it from the hostile ions that were present in the corrosive environment. After the application of inhibitor, the surface roughness was reduced to 589 nm on average, which was suggestive of film growth of the inhibitor across the surface of the mild steel [43-44].

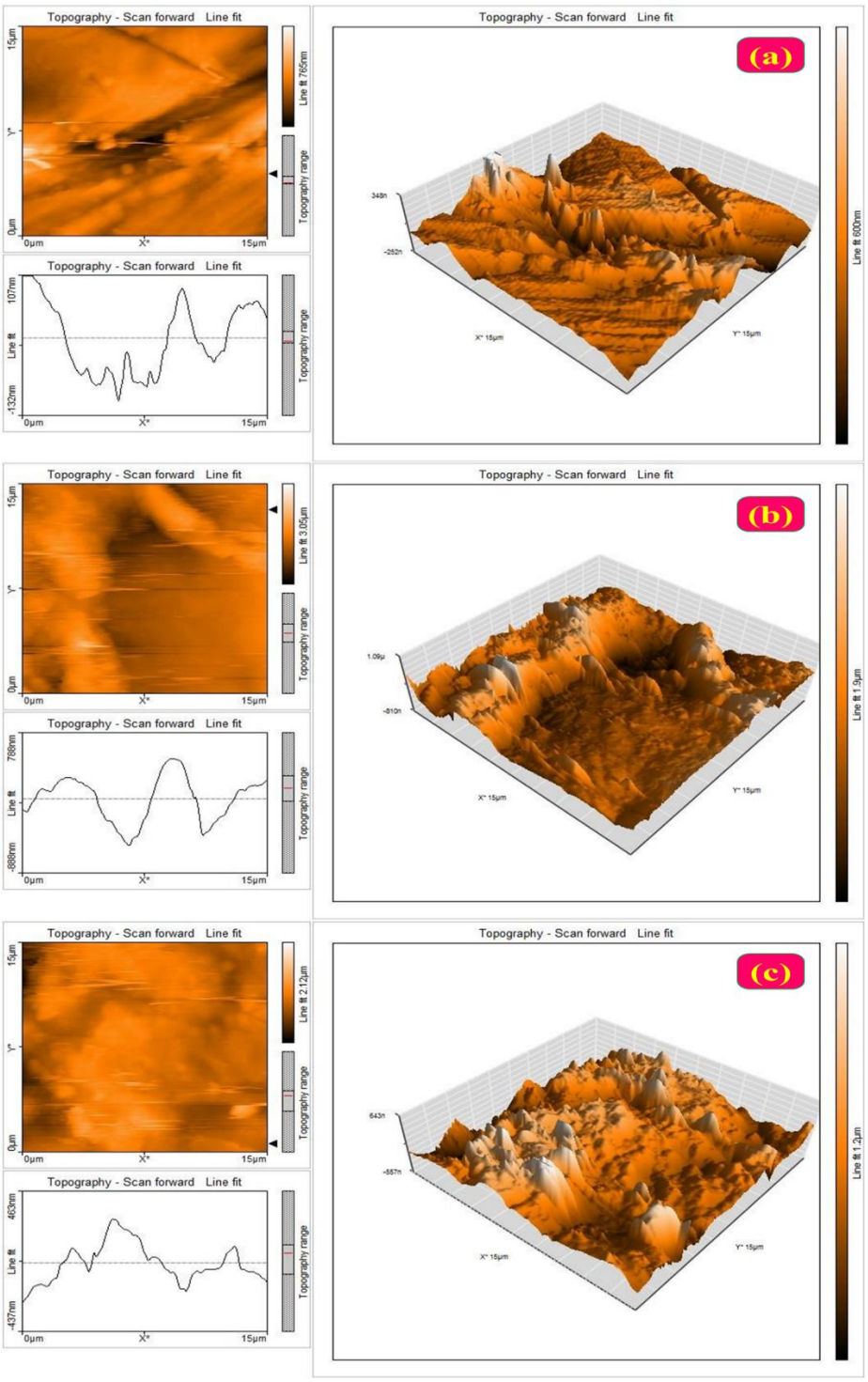

Figure 8 Topological image of (a) Polished mild steel specimen (control), (b) Mild steel specimen immersed in sea water, (c) Mild steel specimen immersed in sea water with inhibitor (2-(benzylidene amino)-benzenethiol) Spectra.

Table 4

Topological analysis for mild steel immersed in the presence and absence of inhibitor systems

Samples	Value in (nm)			
	S_p	S_q.	S_a	S_y
Polished mild steel	85.65	20.21	16.2	162.21
Polished mild steel + sea water	1315	277.53	217.24	2348
Polished mild steel + sea water + 250 ppm of 2-(benzylidene-amino)- benzenethiol	241.3	61.74	47.21	544.7

4.Conclusion

The current study is to use the corrosion inhibitor 2-(benzylidene-amino)-benzenethiol to avert the corrosion of mild steel submerged in sea water solution. Increase in inhibition efficiency and decrease in corrosion rate of MS in sea water medium was observed with the increase in concentration of inhibitor. The maximum inhibition efficiency of 82.37% was achieved for 250 ppm of organic compound as corrosion inhibitor. Based on the findings from the weight-loss method, the polarisation research, AC impedance measurements, and surface examination methods including FTIR spectroscopy and Scanning Electron Microscopy, the mechanistic components of corrosion inhibition are provided. The rate of corrosion decreases with increased addition of organic compounds, likely as a result of the 2-(benzylidene-gradual amino)-benzenethiol's adsorption on the surface of mild steel. It was discovered that the optimum inhibitory efficiency was 82.37%. FTIR spectra show that the protective layer is composed of Fe^{2+}-2-(benzylidene-amino)-benzenethiol complex, indicating that the inhibitor is mixed type. SEM micrographs reveal the mild steel's surface's smoothness, similar to polished mild steel. EDAX has been used to examine the elemental content of polished mild steel, mild steel submerged in sea water, and mild steel submerged in sea water with inhibitor. The AFM microscopes attest to the mild steel surface's smoothness and roughness. The outcome of the study may find application in processing cotton fabric, metal cleaning and processing, oxide coating, electroplating, electrolytic extraction and wherever aqueous solution containing chloride ions.

Acknowledgement
The authors are thankful to the Principal of Thanthai Periyar Government Arts and Science College (Autonomous), for providing necessary facilities. The authors are also thankful to Principal and College Management Committee Members of Jamal Mohamed College (Autonomous), DBT and DST-FIST, for providing instrumental facilities to carry out research work.

Reference

1. Ayoola, A. A., Babalola, R., Durodola, B. M., Alagbe, E. E., Agboola, O., And Adegbile, E. O. *Results in Engineering*, **2022** ,15, 100490.
2. Koundal, M., Singh, A. K., And Sharma, C. *Journal of Molecular Liquids*, **2022**. *350*, 118561.
3. Hassan, N., Ramadan, A. M., Khalil, S., Ghany, N. A. A., Asiri, A. M., And El-Shishtawy, R. M. Colloids and Surfaces A: Physicochemical and Engineering Aspects, **2020**, 607, 125454.
4. Ahangar, M., Izadi, M., Shahrabi, T., And Mohammadi, I. *Journal of Molecular Liquids*, **2020**, *314*, 113617.
5. Pareek, S., Jain, D., Behera, D., Sharma, S., And Shrivastava, R. (). Materials Today: Proceedings, **2021** ,43, 3303-3308..
6. Diraki, A., And Omanovic, S.*Progress in Organic Coatings*, **2022**,. *168*, 106835.
7. Duboscq, J., Sabot, R., Jeannin, M., And Refait, P. . *Materials and corrosion*, **2019**, *70*(6), 973-984.
8. Abdelshafeek, K. A., Abdallah, W. E., Elsayed, W. M., Eladawy, H. A., And El-Shamy, A. M. *Scientific Reports*, **2022**, *12*(1), 20611
9. Atan, F., Rosliza, R., and Syahidah, W. W. The efficiency of moringa leaf (Moringa Oleifera) as green material carbon steel corrosion inhibitor for different concentration of sea water. In *Journal of Physics: Conference Series* ,**2022**,2266(1), 012009).
10. Gao, Y., Ward, L., Fan, L., Li, H., And Liu, Z. ,*Journal of Molecular Liquids*, **2019**, *294*, 111634.
11. Sheit, H. M. K., Mubarak, M. S., and Benitta, G. *Journal of Bio-and Tribo-Corrosion*,**2022**,*8*(4), 103.
12. Raja, T., Abuthahir, S. S., Vijaya, K., and Vijayakumar, P.. *European Journal of Molecular and Clinical Medicine*, **2022**. *9*(08),

13. Bokati, K. S., Dehghanian, C., and Yari, S. *Corrosion Science*, **2017**,*126*, 272-285.
14. Ramezanzadeh, M., Bahlakeh, G., And Ramezanzadeh, B. *Journal of Molecular Liquids*, **2019**. *292*, 111387.
15. Dr. Yabesh Abraham Durairaj Isravel, "Analysis of Ethical Aspects Among Bank Employees with Relation to Job Stratification Level" Eur. Chem. Bull. 2023, 12(Special Issue 4), 3970-3976.
16. Thakur, A., Kaya, S., Abousalem, A. S., Sharma, S., Ganjoo, R., Assad, H., And Kumar, A. *Process Safety and Environmental Protection*, **2022**. *161*, 801-818.
17. Al-Rashed, O., and Abdel Nazeer, A.*Materials*, . **2022**,*15*(6), 2326.
18. Pour-Ali, S., And Hejazi, S.. *Journal of Molecular Liquids*,**2022**, *354*, 118886.
19. Mobin, M., Aslam, R., Salim, R., And Kaya, S. *Journal of Colloid and Interface Science*, **2022**, *620*, 293-312.
20. Lawal, O. J., Potgieter, J. H., Billing, C., And Whitefield, D. J.*Minerals*, **2022 ,**12(4), 416.
21. El Azzouzi, M., Azzaoui, K., Warad, I., Hammouti, B., Shityakov, S., Sabbahi, R.,and Zarrouk, A. *Journal of Molecular Liquids*, **2022,***347*, 118354.
22. Koundal, M., Singh, A. K., And Sharma, C. *Journal of Molecular Liquids*,**2022**, *350*, 118561.
23. Abbas, M. A., Ismail, A. S., Zakaria, K., El-Shamy, A. M., And El Abedin, S. Z. *Scientific Reports*, **2022**, *12*(1), 12536.
24. Kaya, F., Solmaz, R., And Geçibesler, İ. H. *Journal of Molecular Liquids*,**2023** ,121219.
25. Kamaruzzaman, W. M. I. W. M., Shaifudin, M. S., Nasir, N. A. M., Hamidi, N. A. S. M., Yusof, N., Adnan, A., ... And Ghazali, M. S. M. *Journal of Materials Research and Technology*, **2022**,*21*, 3815-3827.
26. Atan, F., Rosliza, R., And Syahidah, W. W. *Journal of Physics: Conference Series*,***2022*** ,2266(1), 012009.
27. Rajendran, D., Sasilatha, T., Rajendran, S. S., Al-Hashem, A., Lačnjevac, Č., and Singh, G.*Materials Protection*,**2022** ,*63*(1), 23-36.
28. Raja, T., And Abuthahir, S. S. *Materials Today: Proceedings*,**2022**, *69*, 1501-1508.
29. Vorobyova, V., Skiba, M., And Gnatko, E. *South African Journal of Chemical Engineering*, **2023** ,*43*, 273-295.
30. Chen, T., Chen, M., And Fu, C. *Journal of Applied Polymer Science*,**2022** ,*139*(15), 51922.

31. Haddadi, S. A., Alibakhshi, E., Bahlakeh, G., Ramezanzadeh, B., And Mahdavian, M. *Journal of molecular liquids*,**2019**, *284*, 682-699.
32. Tehrani, M. E. H. N., Ramezanzadeh, M., And Ramezanzadeh, B. *Corrosion Science*, **2021** ,*184*, 109383.
33. Ralkhal, S., Shahrabi, T., And Ramezanzadeh, B. *Construction and Building Materials*, **2019**,*222*, 400-413.
34. Javadian, S., Darbasizadeh, B., Yousefi, A., Ektefa, F., Dalir, N., and Kakemam, J. *Journal of the Taiwan Institute of Chemical Engineers*, **2017** ,*71*, 344-354.
35. Lei, Y., Qiu, Z., Tan, N., Du, H., Li, D., Liu, J., and Chang, X. *Progress in Organic Coatings*, **2020** ,*139*, 105430.
36. Zhang, W., Li, H. J., Chen, L., Sun, J., Ma, X., Li, Y.,and Wu, Y. C. *Desalination*, **2020**,*486*, 114482.
37. Bokati, K. S., Dehghanian, C., And Yari, S.. *Corrosion Science*, **2017**, *126*, 272-285.
38. Zeino, A., Abdulazeez, I., Khaled, M., Jawich, M. W., And Obot, I. B. *Journal of Molecular Liquids*,**2018**, *250*, 50-62.
39. Zakir Hossain, S. M., Kareem, S. A., Alshater, A. F., Alzubair, H., Razzak, S. A., and Hossain, M. M. *Arabian Journal for Science and Engineering*,**2020**, *45*, 229-239.
40. Bahlakeh, G., Dehghani, A., Ramezanzadeh, B., And Ramezanzadeh, M. *Journal of Molecular Liquids*, **2019**,*294*, 111550.
41. Dehghani, A., Poshtiban, F., Bahlakeh, G., and Ramezanzadeh, B. *Construction and Building Materials*,**2020**, *239*, 117812.
42. Palaniappan, N., Cole, I., Caballero-Briones, F., Manickam, S., Thomas, K. J., and Santos, D. *RSC advances*,**2020**, *10*(9), 5399-5411.
43. Farahmand, R., Sohrabi, B., Ghaffarinejad, A., And Meymian, M. R. Z. *Corrosion Science*,**2018**, *136*, 393-401.
44. Boshkova, N., Kamburova, K., Radeva, T., Simeonova, S., Grozev, N., Shipochka, M., And Boshkov, N. *Coatings*,**2022**, *12*(12), 1798.
45. Mofidabadi, A. H. J., Dehghani, A., And Ramezanzadeh, B. *Journal of Molecular Liquids*, **2022**,*346*, 117086.